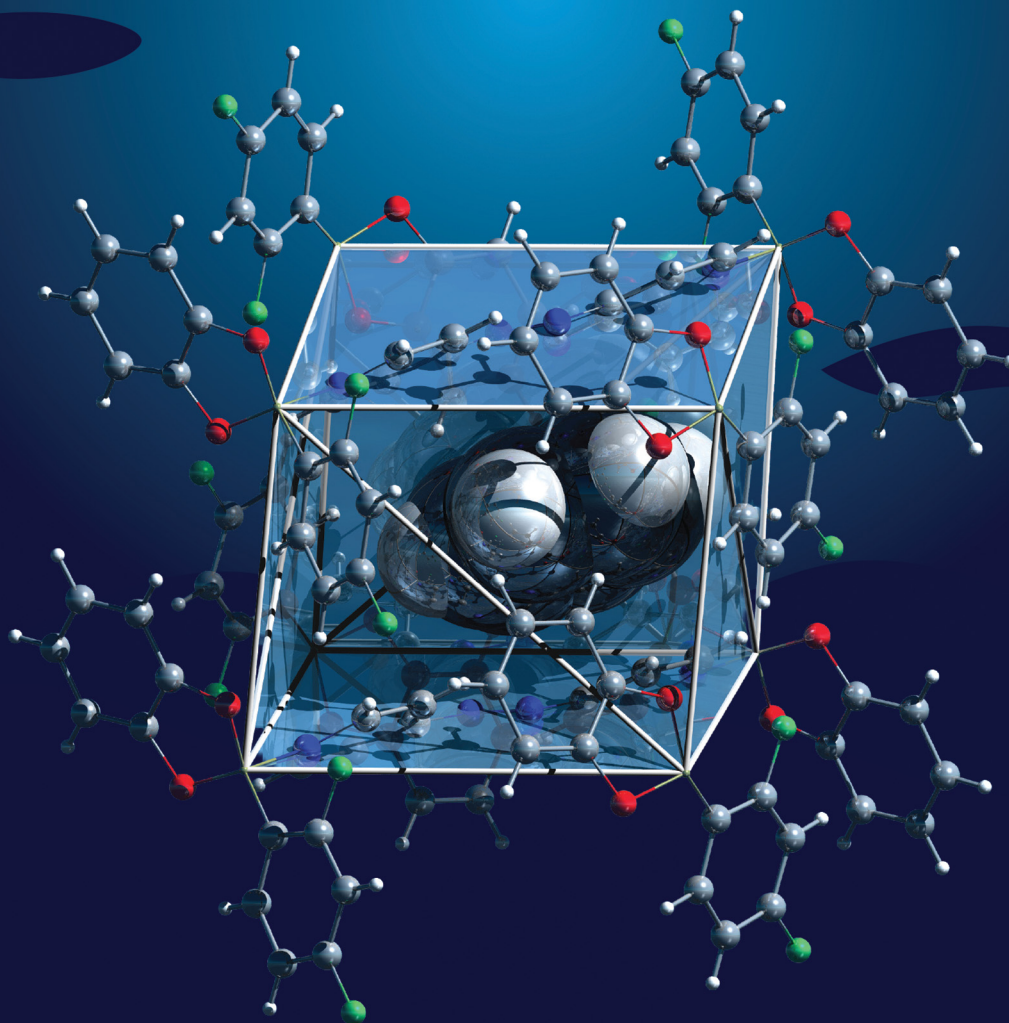


# ChemComm

Chemical Communications

rsc.li/chemcomm



ISSN 1359-7345

**COMMUNICATION**

Gonzalo Campillo-Alvarado, Leonard R. MacGillivray *et al.*  
Rotisserie-like motion enables guest transport in a  
nonporous organic crystal involving a diboron host


 Cite this: *Chem. Commun.*, 2026, 62, 4519

 Received 18th September 2025,  
Accepted 13th January 2026

DOI: 10.1039/d5cc05394c

rsc.li/chemcomm

## Rotisserie-like motion enables guest transport in a nonporous organic crystal involving a diboron host

 Gonzalo Campillo-Alvarado,<sup>a</sup> Eva C. Vargas-Olvera,<sup>b</sup> Dale C. Swenson,<sup>c</sup> Hugo Morales-Rojas,<sup>b</sup> Herbert Höpfl<sup>b</sup> and Leonard R. MacGillivray<sup>b,cd</sup>

We describe a nonporous organic crystal that exhibits a single-crystal-to-single-crystal (SCSC) desolvation. The crystal is based on a boron host that contains an azopyridyl linker. The molecules in the single crystal exhibit novel rotisserie-like movement upon guest release (*i.e.* benzene) that involves (i) rotation and (ii) stretching of the azopyridyl axle, and (iii) tilting of a boronic ester wheel. A crystalline intermediate isolated supports the rotisserie-style movement of the host.

The advent of synthetic molecular machines (MMs) has been accompanied by an increased understanding of molecular dynamics. Collective molecular motions encoded in MMs (*e.g.* anisotropic rotation,<sup>1</sup> alkene isomerization and translation) are key features to develop MMs that function in crystalline solids. While motion has been attained in a variety of porous and robust frameworks constructed by metal-organic materials,<sup>2</sup> understanding and developing molecular movements in close-packed organic crystals remains a fundamental challenge owing to losses of structural integrity (*i.e.* crystallinity) that are often triggered by guest release.<sup>3</sup>

In this context, X-ray diffraction (XRD) analyses of single-crystal-to-single-crystal transformations (SCSCs) can offer unambiguous mechanistic insights into structural changes from which molecular motions in crystalline solids can be attributed before and after physical or chemical stimuli.<sup>4</sup> SCSCs have shed light on movements involving rotations,<sup>5</sup> [2 + 2]-photodimerizations,<sup>6</sup> photocyclizations,<sup>7</sup> *cis-trans* isomerizations,<sup>8</sup> polymorphic transformations,<sup>9</sup> and host-guest (HG) behaviours

(*e.g.* solvent exchange, desolvation).<sup>10</sup> For the latter, mechanisms of guest transport in purely organic solids while becoming more prevalent,<sup>11</sup> remain generally poorly understood with particularly only a few examples documented in close-packed organic crystals.<sup>12</sup>

While the HG chemistry of diboron compounds such as **S** is advancing rapidly, examples involving both SC transformation and guest release involving nonporous boron solids are currently unknown. A recent study reported visible light-induced guest release in a boron solid through weakened HG interactions mediated by a [2 + 2] photocycloaddition of boroxines. However, the process did not proceed through an SC desolvation (Scheme 1).<sup>13</sup>

Herein, we report a purely organic crystal HG system that facilitates guest transport through a nonporous lattice (Scheme 1a). Specifically, we demonstrate the diboron host (**S**) to undergo a rearrangement in the crystal lattice (**D**) to facilitate release of entrapped guest molecules (*i.e.* benzene) without loss of crystal integrity (Scheme 1b). We identify a mechanism by which guest transport occurs *via* SCSC desolvation. The mechanism is reminiscent of the motion of a macroscopic rotisserie and consists of collective motions involving: (i) rotation of a bipyridyl linker, (ii) elongation or stretching of the host, and (iii) tilting of stator units. The rotisserie-style guest transport mechanism in the single crystal is supported by the isolation of a crystalline intermediate (**I**) of the host (Scheme 1c). Pioneering work of Atwood demonstrated nonporous crystals based on bowl-shaped calixarenes to undergo SCSC desolvation.<sup>14</sup> The resilience of the SC character of the material was rationalized by cooperativity of weak dispersive forces that facilitate guest transport through the crystal without disrupting the overall structure and SC character. Guest transport in nonporous close-packed crystals, being of much current interest in solid state and materials chemistry, is still exemplified by only very few examples.<sup>11,12,15</sup>

A nonporous organic and dynamic solid is realized here by assembly of 2,4-trifluorophenylboronic acid catechol ester (**1**)

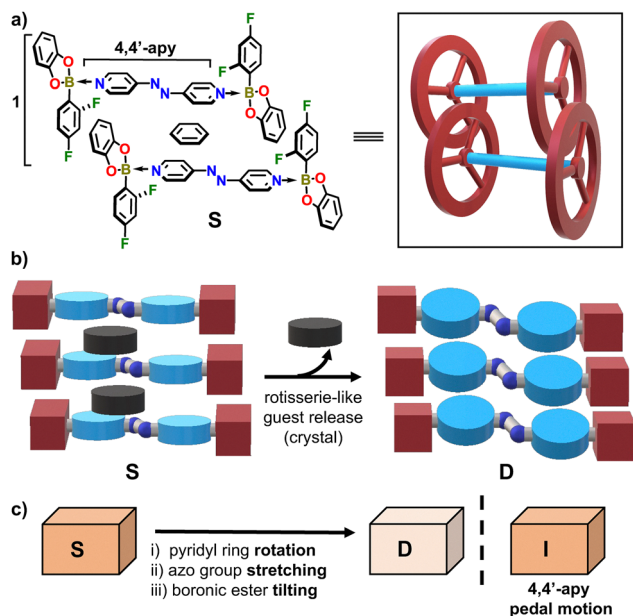
<sup>a</sup> Department of Chemistry, Reed College, Portland, OR 97202-8199, USA.  
E-mail: gcampillo@reed.edu

<sup>b</sup> Centro de Investigaciones Químicas, Instituto de Investigación en Ciencias Básicas y Aplicadas, Universidad Autónoma del Estado de Morelos, Av. Universidad 1001, Cuernavaca, 62209, México

<sup>c</sup> Department of Chemistry, University of Iowa, Iowa City, Iowa 52242, USA.  
E-mail: Leonard.Macgillivray@usherbrooke.ca

<sup>d</sup> Département de Chimie, Université de Sherbrooke, Sherbrooke, QC, J1K 2R1, Canada





**Scheme 1** Design and desolvation mechanism of diboron HG **S**: (a) Diboron HG **S**, (b) collective rotisserie-style desolvation of **S**, and (c) individual molecular movements (**S**: solvated; **D**: desolvated; **I**: intermediate).

and 4,4'-azopyridine (**4,4'-apy**)<sup>16</sup> in the presence of benzene.<sup>17</sup> The assembly process affords the crystalline solid **S** of composition  $2(1) \cdot (4,4'\text{-apy}) \supset \text{C}_6\text{H}_6$ . Intrinsic dynamic behaviour of the central  $\text{N}=\text{N}$  bond of **4,4'-apy** to exhibit pedal motion coupled with flexibility of the  $\text{B} \leftarrow \text{N}$  bond promotes guest transport.

The components of **S** crystallize as dark-red prisms in the monoclinic space group  $P2_1/c$  (Fig. 1).  $\text{B} \leftarrow \text{N}$  coordination involving **4,4'-apy** (1.665(6) Å) produces a diboron adduct akin to a wheel-and-axle structure. The bipyridine **4,4'-apy** serves as the axle with the  $\text{B} \leftarrow \text{N}$  bonds providing connection to the wheels. The axles are coplanar with the distance between the wheels ( $\text{N}_{\text{pyr}} \cdots \text{N}_{\text{pyr}}$ ) on the order of 8.939(6) Å (torsion angle: 29°). The coplanarity is in agreement with a majority of conformations of 4,4'-azopyridines in the solid state.<sup>18</sup> The wheel-and-axle assemblies pack into layers connected by interdigitated wheel-to-wheel interactions. Importantly, the crystal accommodates encapsulated benzene molecules (23.6% unit cell volume) that form face-to-face  $\pi \cdots \pi$  interactions (Table S2) with the axles (Fig. 1a). Four adjacent host adducts interact orthogonally with the benzene by weak  $\text{C-H} \cdots \pi$  forces in the  $bc$ -plane to completely encapsulate the guests in an enclosed cavity. The topology of the cavity conforms to a distorted square prism as defined by distances between adjacent boron atoms (Fig. 1b). Layers of boron hosts pack parallel to the  $c$ -axis wherein the guests occupy the enclosed polyhedral space (Fig. 1c).

While the benzene molecules are completely enclosed in polyhedral cavities of **S**, the benzene guests escape from the crystals in a rare SCSC transformation that generates **D**. The loss of benzene is spontaneous, occurring at ambient temperature and pressure. A SCXRD analysis of **D** reveals complete loss of electron density in the enclosed cavities. The loss of the

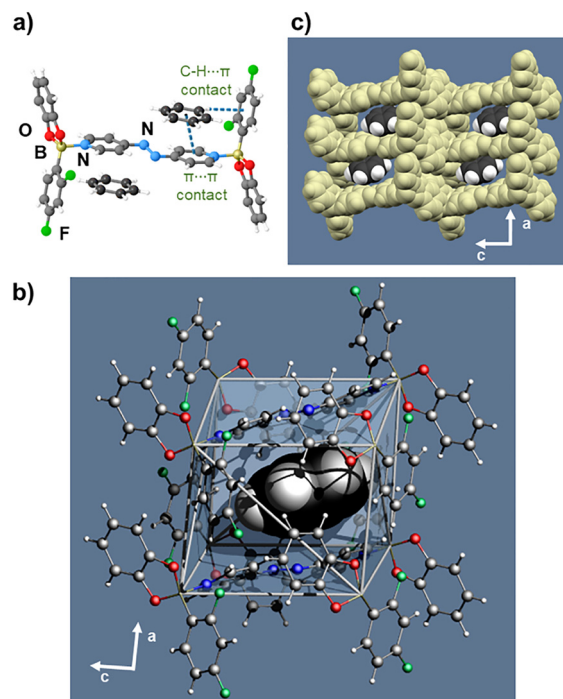


**Fig. 1** X-ray structure of solvated host **S**: (a) face-to-face  $\pi$ -stacks of diboron adduct with encapsulated benzene, (b) polyhedral cavity encloses benzene, (c) sheet packing along the  $c$ -axis.

benzene was accompanied by the unit cell transforming into the monoclinic space group  $P2_1/n$ . A close comparison of the unit cell dimensions of **S** and **D** shows an appreciable reduction of the cell volume (281.43 Å<sup>3</sup> or 15.4%) with shortenings of all cell axes and increase of the  $\beta$  angle (10.2°) (Table S1).

Thermogravimetric (TG) and differential scanning calorimetry (DSC) experiments (Fig. S4 and S5) of single crystals of **S** showed a desolvation onset at 81.6 °C accompanied by a mass loss of 11.1%. The desolvation is in agreement with the benzene content of **S**. Partial sublimation of the sample (84.2% mass loss) occurred at 166.9 °C. These observations provide unambiguous evidence of conditions for guest loss.<sup>14</sup>

A detailed crystallographic analysis confirmed the composition of **D** as  $2(1) \cdot (4,4'\text{-apy})$  (Fig. 2). A single molecule of **1** is coordinated to one-half of **4,4'-apy**. The  $\text{B} \leftarrow \text{N}$  bond length (1.681(6) Å) and  $\text{N}_{\text{pyr}} \cdots \text{N}_{\text{pyr}}$  distance (8.999(7) Å) of the coplanar axle increased while the  $\text{N}=\text{N}$  bond displays criss-cross disorder (Fig. 2a and b).<sup>19</sup> A combination of torsion of the **4,4'-apy** axle (37.3°) and tilting of the boron wheel (19.1°) (Fig. 2c) resulted in face-to-face  $\pi \cdots \pi$  stacks of adjacent hosts (Fig. 2d and Table S2). We attribute molecular reorientation of the host in the SC to facilitate transport and escape of the guest benzene molecules. Cooperative loss of the benzene guests likely occurred without formation of channels expected to disrupt crystallinity of the close-packed solid as shown by extended packing and inter-adduct distances (Fig. S1–S3). We note the loss of benzene was determined to be irreversible.

Insight into the nature of the cooperative motion is provided by the isolation of a single-crystalline phase **I** that was present



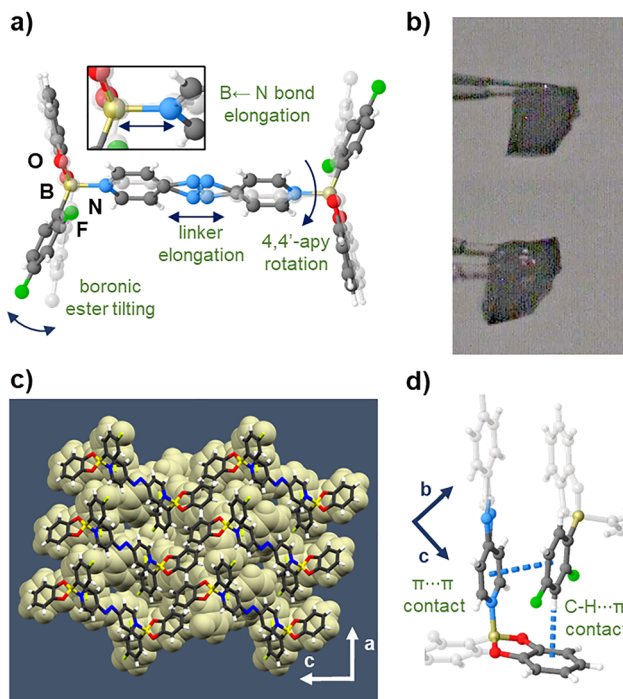


Fig. 2 X-ray structure of desolvated host **D**: (a) overlay with diboron host **S** (grey), (b) single crystal before (above) and after (below) benzene escape, (c), extended view in *ac*-plane, and (d) interactions formed during benzene escape.

in the same vial as **S** as red prisms. SCXRD and  $^1\text{H}$  NMR spectroscopy confirmed **S** as  $2(\mathbf{1}) \cdot (\mathbf{4,4}'\text{-apy}) \supset 0.5(\text{C}_6\text{H}_6)$ . Given that phase **I** differs from phase **S** based on stoichiometry of the included benzene solvent, phase **I** is a pseudo-polymorph of **S** and likely an intermediate from  $\text{S} \rightarrow \text{D}$ .<sup>20</sup>

The components of **I** crystallize in the monoclinic space group  $P2_1/c$ . The asymmetric unit contains two wheels (**1**) connected to an axle ( $\mathbf{4,4}'\text{-apy}$ ) through  $\text{B} \leftarrow \text{N}$  bonds [1.672(5) and 1.650(5) Å] (Fig. 3a). The pyridyl rings of the axle exhibit a large twist angle ( $46.6^\circ$ ) along the flexible  $\text{N}=\text{N}$  bond unit.<sup>21</sup> The  $\text{N}_{\text{pyr}} \cdots \text{N}_{\text{pyr}}$  distance (8.975(4) Å) situates between **S** and **D**. The benzene guests (13.5% unit cell volume) of **I** form edge-to-face *versus* face-to-face  $\pi \cdots \pi$  interactions with  $\mathbf{4,4}'\text{-apy}$  as compared to **S**. Collectively, the dynamic and cooperative interactions of the components in **S**, **D** and **I** provide insight into a capacity of the components to undergo complex and cooperative dynamics considered underpinnings of crystalline MMs. From the structure of the intermediate **I**, we postulate a rotisserie-style motion likely defines the cooperative movement to facilitate guest transport/escape without concomitant formation of channels and loss of mosaicity of the SC. Indeed, optimized geometries of the diboron adducts of **S** and **I** closely match that of **D**, supporting a rotisserie-style molecular reorientation (Fig. S6). The reorientations are accompanied by energetic gains of  $-19.88$  and  $-7.39$  kcal mol $^{-1}$  for **S** and **I**, respectively (Table S3).

In summary, we have discovered a solid-state mechanism of desolvation from a boron host in a close-packed organic crystal by means of X-ray crystallography. The ability of the molecular

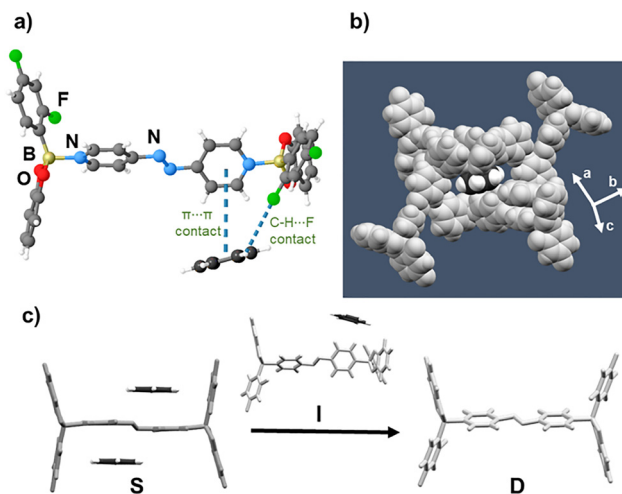


Fig. 3 X-ray structure of pseudo-polymorph host **I**: (a)  $\pi \cdots \pi$  and  $\text{C-H} \cdots \text{F}$  contacts of adduct with benzene, (b) confinement of benzene, (c) comparison with molecular geometries of **S** and **D**.

structure of the host to engage in rotisserie-style motion facilitates guest transport and release while retaining crystallinity. Given emerging interests in the development of molecular machinery where there are now transitions from conceptual stages to applications (*i.e.* serviceable machine), we expect the rotisserie-style mechanism evoked here to be regarded as a model to add to the toolbox of dynamics in single crystals (*e.g.*, amphidynamic crystals or rigid lattice with moving parts),<sup>5a,22</sup> which contains rotor-like molecular analogs (*i.e.*, gyroscope, brake, propeller). Implications are that equipping organic molecules in close-packed crystalline solids that display host-guest capacity with a motion-generating unit can relay the mobility of guests through a lattice without disruption of the crystal character. While the desolvation here is not reversible, the results highlight potential pathways to enable guests to traverse interiors of non-porous solids, with implications for the design of smart molecular sensors or actuators.<sup>23</sup> It is reasonable to expect that the motion can be effectively incorporated into functional solids based on dynamic organic systems.

We gratefully acknowledge the National Science Foundation (LRM DMR-1708673, GC-A CHE-2319929) and Reed College for financial support.

## Conflicts of interest

There are no conflicts to declare.

## Data availability

The datasets supporting this article have been uploaded as part of the supplementary information (SI). Supplementary information: experimental information, TG-DSC patterns, and additional SCXRD data. See DOI: <https://doi.org/10.1039/d5cc05394c>.

CCDC 1998621–1998623 contain the supplementary crystallographic data for this paper.<sup>24a–c</sup>



## References

- 1 L. Catalano and P. Naumov, *CrystEngComm*, 2018, **20**, 5872–5883.
- 2 W. Danowski, T. van Leeuwen, S. Abdolazadeh, D. Roke, W. R. Browne, S. J. Wezenberg and B. L. Feringa, *Nat. Nanotechnol.*, 2019, **14**, 488–494.
- 3 (a) I. Roy and J. F. Stoddart, *Trends Chem.*, 2019, **1**, 627–629; (b) S. P. Yelgaonkar, G. Campillo-Alvarado and L. R. MacGillivray, *J. Am. Chem. Soc.*, 2020, **142**, 20772–20777.
- 4 (a) P. Naumov and P. K. Bharadwaj, *CrystEngComm*, 2015, **17**, 8775; (b) A. Chaudhary, A. Mohammad and S. M. Mobin, *Cryst. Growth Des.*, 2017, **17**, 2893–2910; (c) M. A. Garcia-Garibay, *Angew. Chem., Int. Ed.*, 2007, **46**, 8945–8947; (d) W. M. Awad, D. W. Davies, D. Kitagawa, J. Mahmoud Halabi, M. B. Al-Handawi, I. Tahir, F. Tong, G. Campillo-Alvarado, A. G. Shtukenberg, T. Alkhidir, Y. Hagiwara, M. Almehairbi, L. Lan, S. Hasebe, D. P. Karothu, S. Mohamed, H. Koshima, S. Kobatake, Y. Diao, R. Chandrasekar, H. Zhang, C. C. Sun, C. Bardeen, R. O. Al-Kaysi, B. Kahr and P. Naumov, *Chem. Soc. Rev.*, 2023, **52**, 3098–3169.
- 5 (a) C. S. Vogelsberg and M. A. Garcia-Garibay, *Chem. Soc. Rev.*, 2012, **41**, 1892–1910; (b) A. Colin-Molina, D. P. Karothu, M. J. Jellen, R. A. Toscano, M. A. Garcia-Garibay, P. Naumov and B. Rodriguez-Molina, *Matter*, 2019, **1**, 1033–1046.
- 6 (a) Q. Chu, D. C. Swenson and L. R. MacGillivray, *Angew. Chem., Int. Ed.*, 2005, **44**, 3569–3572; (b) G. Campillo-Alvarado, C. Li, Z. Feng, K. M. Hutchins, D. C. Swenson, H. Höpfl, H. Morales-Rojas and L. R. MacGillivray, *Organometallics*, 2020, **39**, 2197–2201; (c) S. Bhandary, R. Shukla, A. M. Kaczmarek and K. Van Hecke, *Acc. Chem. Res.*, 2025, **58**, 2724–2736; (d) S. Bhandary, M. Beliš, R. Shukla, L. Bourda, A. M. Kaczmarek and K. Van Hecke, *J. Am. Chem. Soc.*, 2024, **146**, 8659–8667.
- 7 S. Kobatake, S. Takami, H. Muto, T. Ishikawa and M. Irie, *Nature*, 2007, **446**, 778–781.
- 8 O. S. Bushuyev, A. Tomberg, T. Friščić and C. J. Barrett, *J. Am. Chem. Soc.*, 2013, **135**, 12556–12559.
- 9 T. N. Drebuschak, V. A. Drebuschak, N. A. Pankrushina and E. V. Boldyreva, *CrystEngComm*, 2016, **18**, 5736–5743.
- 10 M. Kawano and M. Fujita, *Coord. Chem. Rev.*, 2007, **251**, 2592–2605.
- 11 R. M. Payne and C. L. Oliver, *CrystEngComm*, 2016, **18**, 7965–7971.
- 12 S. Bhandary and D. Chopra, *Cryst. Growth Des.*, 2018, **18**, 27–31.
- 13 J. Xu, T. Wang, S. Deng, W. Lai, Y. Shi, Y. Zhao, F. Huang and P. Wei, *Angew. Chem., Int. Ed.*, 2024, **63**, e202411880.
- 14 J. L. Atwood, L. J. Barbour, A. Jerga and B. L. Schottel, *Science*, 2002, **298**, 1000–1002.
- 15 (a) P. K. Thallapally, G. O. Lloyd, J. L. Atwood and L. J. Barbour, *Angew. Chem.*, 2005, **117**, 3916–3919; (b) J. A. Riddle, J. C. Bollinger and D. Lee, *Angew. Chem., Int. Ed.*, 2005, **44**, 6689–6693; (c) K. Nakano, K. Sada, K. Nakagawa, K. Aburaya, N. Yoswathananont, N. Tohna and M. Miyata, *Chem. – Eur. J.*, 2005, **11**, 1725–1733; (d) Y. Li, M. Handke, Y.-S. Chen, A. G. Shtukenberg, C. T. Hu and M. D. Ward, *J. Am. Chem. Soc.*, 2018, **140**, 12915–12921.
- 16 (a) K. M. Hutchins, D. K. Unruh, F. A. Verdu and R. H. Groeneman, *Cryst. Growth Des.*, 2018, **18**, 566–570; (b) P. Gupta, D. P. Karothu, E. Ahmed, P. Naumov and N. K. Nath, *Angew. Chem.*, 2018, **130**, 8634–8638.
- 17 (a) G. Campillo-Alvarado, E. C. Vargas-Olvera, H. Höpfl, A. D. Herrera-España, O. Sánchez-Guadarrama, H. Morales-Rojas, L. R. MacGillivray, B. Rodriguez-Molina and N. Farfan, *Cryst. Growth Des.*, 2018, **18**, 2726–2743; (b) G. Campillo-Alvarado, K. P. D'mello, D. C. Swenson, S. V. Santhana Mariappan, H. Höpfl, H. Morales-Rojas and L. R. MacGillivray, *Angew. Chem., Int. Ed.*, 2019, **58**, 5413–5416; (c) G. Campillo-Alvarado, M. M. D'mello, M. A. Sinnwell, H. Höpfl, H. Morales-Rojas and L. R. MacGillivray, *Front. Chem.*, 2019, **7**, 695; (d) A. D. Herrera-España, H. Höpfl and H. Morales-Rojas, *ChemPlusChem*, 2020, **85**, 548–560; (e) A. J. Stephens, R. Scopelliti, F. F. Tirani, E. Solari and K. Severin, *ACS Mater. Lett.*, 2019, **1**, 3–7; (f) I. J. Jupiter, J. D. Loya, N. Lutz, P. M. Sittinger, E. W. Reinheimer and G. Campillo-Alvarado, *Cryst. Growth Des.*, 2024, **24**, 5883–5888; (g) A. Shaw, I. Bondarenko, V. Bhaniramka, M. A. West, P. F. Gilbert, J. D. Loya, C. Li and G. Campillo-Alvarado, *ChemPlusChem*, 2025, **90**, e202500434.
- 18 (a) G. J. Halder, C. J. Kepert, B. Moubaraki, K. S. Murray and J. D. Cashion, *Science*, 2002, **298**, 1762–1765; (b) P. P. Mazzeo, C. Carraro, A. Arns, P. Pelagatti and A. Bacchi, *Cryst. Growth Des.*, 2020, **20**, 636–644.
- 19 (a) X. Ding, D. K. Unruh, L. Ma, E. J. van Aalst, E. W. Reinheimer, B. J. Wylie and K. M. Hutchins, *Angew. Chem., Int. Ed.*, 2023, **62**, e202306198; (b) N. Juneja, D. K. Unruh and K. M. Hutchins, *Chem. Mater.*, 2023, **35**, 7292–7300.
- 20 H. H. Monfared, A.-C. Chamayou, S. Khajeh and C. Janiak, *CrystEngComm*, 2010, **12**, 3526–3530.
- 21 (a) X. Chi, W. Cen, J. A. Queenan, L. Long, V. Lynch, N. M. Khashab and J. L. Sessler, *J. Am. Chem. Soc.*, 2019, **141**, 6468–6472; (b) P. Commins and M. A. Garcia-Garibay, *J. Org. Chem.*, 2014, **79**, 1611–1619.
- 22 M. A. Garcia-Garibay, *Proc. Natl. Acad. Sci. U. S. A.*, 2005, **102**, 10771–10776.
- 23 A. I. Vicatos, L. Loots, G. Mathada, J. Drwęska, A. M. Janiak and L. J. Barbour, *Nat. Mat.*, 2025, DOI: [10.1038/s41563-025-02393-6](https://doi.org/10.1038/s41563-025-02393-6).
- 24 (a) CCDC 1998621: Experimental Crystal Structure Determination, 2025, DOI: [10.5517/ccdc.csd.cc252qnn](https://doi.org/10.5517/ccdc.csd.cc252qnn); (b) CCDC 1998622: Experimental Crystal Structure Determination, 2025, DOI: [10.5517/ccdc.csd.cc252qpp](https://doi.org/10.5517/ccdc.csd.cc252qpp); (c) CCDC 1998623: Experimental Crystal Structure Determination, 2025, DOI: [10.5517/ccdc.csd.cc252qqg](https://doi.org/10.5517/ccdc.csd.cc252qqg).

